Synthesis, crystal structures, and redox behavior of bis(2-phenylindenyl)nickel and bis(2-phenylindenyl)zirconium dichloride

O. N. Babkina,[a] T. A. Bazhenova,[a] N. M. Bravaya,[a] V. V. Strelets,[a]* M. Yu. Antipin,[b]* and K. A. Lysenko[b]*

[a]*Institute of Chemical Physics in Chernogolovka, Russian Academy of Sciences, 142432 Chernogolovka, Moscow Region, Russian Federation. Fax: +7 (096) 515 3588*

[b]*A. N. Nesmeyanov Institute of Organoelement Compounds, Russian Academy of Sciences, 28 ul. Vavilova, 117813 Moscow, Russian Federation. Fax: +7 (095) 135 5085*

Redox reactions of the sandwich $[\eta^5\text{-(Ph)Ind}]_2Ni$ complex (**1**) (where (Ph)Ind is the 2-phenylindenyl anion) in CH_2Cl_2 and of the bent-sandwich $[\eta^5\text{-(Ph)Ind}]_2ZrCl_2$ complex (**2**) in THF have been studied by low-temperature cyclic voltammetry. Complex **1** undergoes quasi-reversible two-step oxidation to cation $\mathbf{1}^+$ and dication $\mathbf{1}^{2+}$, which are stable at room temperature within the cyclic voltammetry time scale. Two-electron reduction of complex **1** is irreversible up to −50 °C, and this process is accompanied by destruction of the sandwich structure of the complex. Reduction of complex **2** is described by the conventional scheme for bent-sandwich complexes. According to this scheme, further one-electron reduction of radical anion $\mathbf{2}^{\cdot -}$ generates dianion $\mathbf{2}^{2-}$, which eliminates two Cl^- ions to afford bisindenyl sandwich complex $[\eta^5\text{-(Ph)Ind}]_2Zr$ (**3**). This complex is stable at $T < -45$ °C within the cyclic voltammetry time scale and is capable of undergoing one-electron reduction to the corresponding radical anion $\mathbf{3}^{\cdot -}$. Synthesis and crystal structures of complexes **1** and **2** are reported.

Key words: metallocene complexes, bis(2-phenylindenyl)nickel, bis(2-phenylindenyl)zirconium dichloride; X-ray structural analysis; cyclic voltammetry; redox properties.

Bis(2-phenylindenyl)zirconium dichloride (**2**) is a highly active stereospecific catalyst for the polymerization of propylene.[1] It should be taken into account that complex **2** may undergo particular electronic changes under the action of alkylation agents that are obligatory components of the catalytic system and that exhibit reduction properties. In this connection, we studied the redox behavior of this complex by cyclic voltammetry in the temperature range from −60 to +15 °C. Two-electron electroreduction of metallocene dichlorides of Groups IV—VI metals is accompanied by elimination of two chloride ions to form the corresponding short-lived sandwich complexes.[2,3] Therefore, electrochemical generation of bis(2-phenylindenyl)zirconium (**3**) would be expected; it is of interest to study its stability and redox properties and to elucidate whether **3** has a sandwich structure. For this purpose, it was necessary to perform a comparative study of the redox behavior of the stable bisindenyl complex, which undoubtedly has a sandwich structure. Among these complexes are bis(indenyl)complexes of Group VIII metals, although not many of these complexes are known.[4,5] In this connection, we synthesized a sandwich complex, namely, bis(2-phenylindenyl)nickel (**1**), which has not previously been reported, and the redox behavior of this complex was studied by cyclic voltammetry. In this work, synthesis and molecular structures of complexes **1** and **2** are also reported.

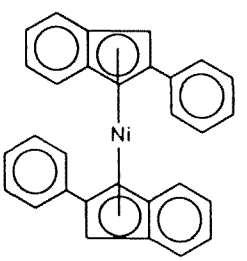

1

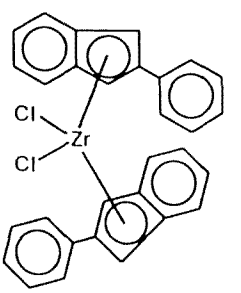

2

Molecular structures of η^5(Ph)Ind]$_2$Ni and $[\eta^5\text{-(Ph)Ind}]_2ZrCl_2$

X-ray structural study of the single crystal of compound **1** demonstrated that in the crystals this compound occurs as an *anti* isomer (Fig. 1). The structure consists of two centrosymmetrical molecules, which are located at two centers of symmetry: (1/2 1/2 0) and

Translated from *Izvestiya Akademii Nauk. Seriya Khimicheskaya*, No. 6, pp. 1529—1536, June, 1996.

1066-5285/96/4506-1458 $15.00

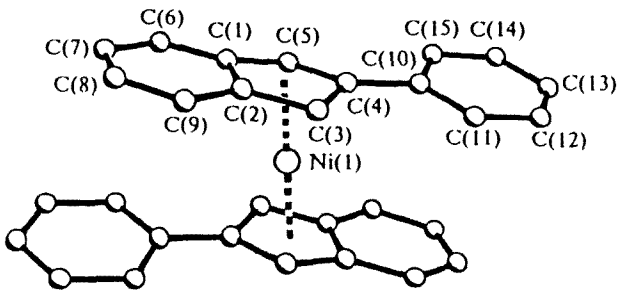

Fig. 1. Molecular structure of $[\eta^5\text{-(Ph)Ind}]_2Ni$.

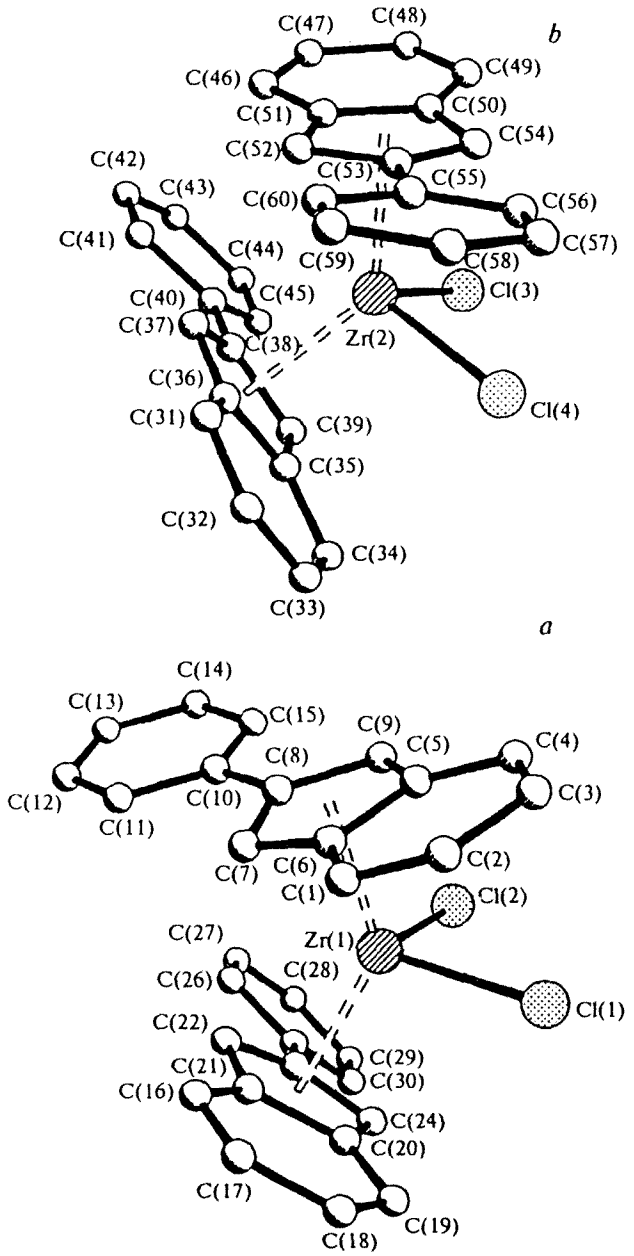

Fig. 2. Molecular structures of (*a*) *syn* and (*b*) *anti* stereoconformers of $[\eta^5\text{-(Ph)Ind}]_2ZrCl_2$.

(1 1 0). The bond lengths and bond angles in two independent molecules are equal within the experimental error. The Ni(1)—X distance, where X is the center of the five-membered ring of the phenylindenyl ligand, is 1.814(7) Å. The five-membered cycles have staggered conformations with C(1)—X(1)—X(2)—C(3A) and C(2)—X(1)—X(2)—C(5A) pseudotorsion angles (X(1) and X(2) are the centers of the five-membered rings) of 37.8(7)° and −36.67(7)°, respectively. The indenyl rings are virtually planar (the rms deviations of the carbon atoms of the ligands are 0.033 Å). The angle between the planes of the phenyl and indenyl rings is 8.5(7)°.

X-ray structural study of a single crystal of the $(2\text{-PhInd})_2ZnCl_2$ compound (**2**) demonstrated that in the crystal, this compound occurs as two rotational isomers (Fig. 2, *a* and *b*) with respect to the Zr—ligand bond (two independent molecules per asymmetric unit).

The molecule of compound **2** is a skewed metallocene with X(1)—Zr(1)—X(2) and X(3)—Zr(2)—X(4) pseudobond angles of 131.2° and 131.6(6)° in two independent molecules, respectively, where X(1)—X(4) are the centers of the five-membered rings of the PhInd ligands. The dihedral angles between the planes of the PhInd ligands are 55.9(7)° and 49.5(9)°.

It should be mentioned that the *syn* and *anti* isomers differ in the mutual rotation of the PhInd ligands. We use the angle at which the long axes of the 2-phenylindenyl ligands (the lines passing through the C(13) atom and the midpoint of the C(2)—C(3) bond and the C(28) atom and the midpoint of the C(17)—C(18) bond in one independent molecule; the C(43) atom and the midpoint of the C(32)—C(33) bond and the C(58) atom and the midpoint of the C(47)—C(48) bond in the second independent molecule) intersect as a value to describe the mutual arrangement of the ligands. The angles between the above-mentioned lines in the *syn* and *anti* isomers (with respect to the Zr—ligand bond) are 35° and 11°, respectively. This difference in the orientation of the ligands is, apparently, determined by the mutual repulsion of the closely-spaced atoms of the phenyl rings in the *syn* isomer. Figure 3 shows projections of the two independent molecules onto the Cl—Zr—Cl plane.

The PhInd five-membered cycles adopt staggered conformations with C(20)—X(1)—X(2)—C(5) and C(39)—X(3)—X(4)—C(50) pseudorotational angles of 35° and 28°, respectively. The 2-phenylindenyl rings are virtually planar (the rms deviations of the carbon atoms of the ligands are in the range 0.112—0.142 Å). The angle between the planes of the phenyl and indenyl cycles in two independent molecules are equal (11.2°) within the experimental error.

In both molecules, the Zr—C distances are in the range 2.467(7)—2.644(7) Å.

The other geometric parameters of structure **2** have standard values. Intermolecular and intramolecular contacts in the structure studied correspond to the typical van der Waals distances.

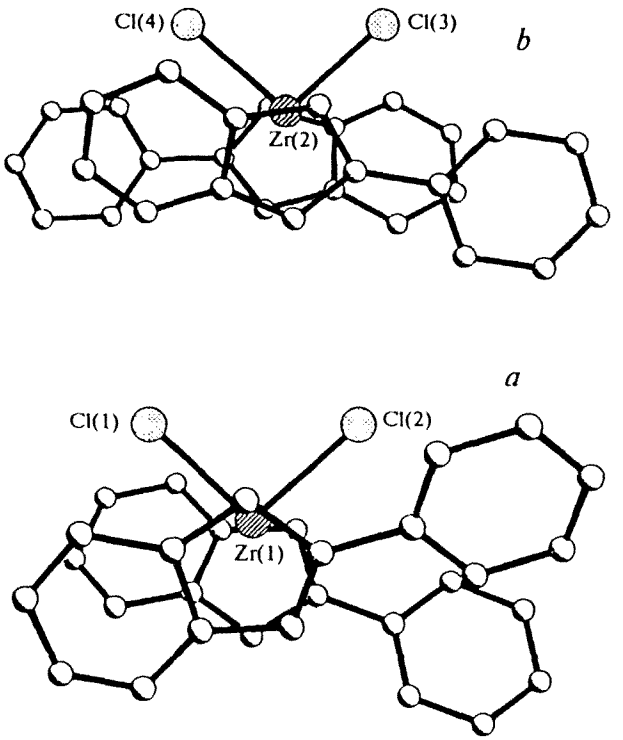

Fig. 3. Projection of the molecular structures of (*a*) *syn* and (*b*) *anti* stereoconformers of $[\eta^5\text{-(Ph)Ind}]_2ZrCl_2$ onto the Cl—Zr—Cl plane.

Electrochemical studies of complexes 1 and 2

Two quasi-reversible one-electron anodic peaks *A* and *B* and one irreversible two-electron cathodic peak *C* are observed in the cyclic voltammograms of the **20ē** $[\eta^5\text{-(Ph)Ind}]_2Ni$ complex (**1**) in CH_2Cl_2 (Fig. 4) throughout the temperature range studied (−50÷+15 °C). The potentials of these peaks are given in Table 1. All peaks observed are diffusion peaks ($I_p \cdot v^{-1/2}$ = const, where I_p is the peak height and v is the rate of the linear potential scan). The peaks were concluded to be one- or two-electron peaks based on a comparison of the heights of peaks *A*, *B*, and *C* with the height of the one-electron peak of the oxidation of dibenzoferrocene[6] when all other factors are the same. The quasi-reversible character of peaks *A* and *B* follows from the equilibrium values of the anode (*A* and *B*) and cathode (*A′* and *B′*) responses and from the values of $\Delta E_p = E^a_p - E^c_p$ = 70–80 mV (where E^a_p and E^c_p are the potentials of anodic and cathodic peaks, respectively) at room temperature. The data obtained makes it possible to represent the redox transformations of complex **1** in the following form:

$$\underset{B/B'}{1^{2+}} \overset{e}{\rightleftharpoons} \underset{A/A'}{1^{+}} \overset{e}{\rightleftharpoons} \underset{C}{1} \overset{2e}{\rightleftharpoons} \text{Product}$$

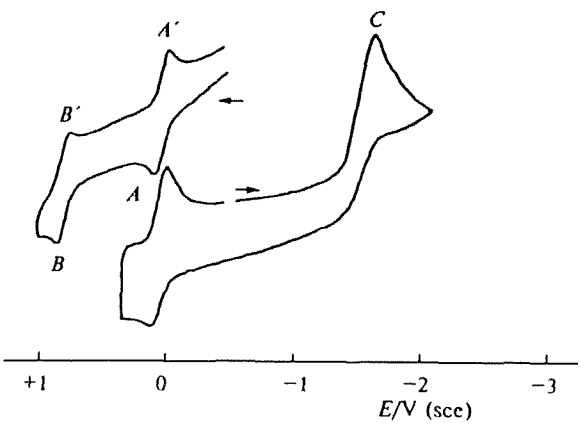

Fig. 4. Cyclic voltammograms of complex **1** ($6.3 \cdot 10^{-4}$ mol L^{-1}) in a CH_2Cl_2 solution/0.05 mol L^{-1} Bu_4NPF_6 on Pt (15 °C) and glassy-carbon (−25 °C) electrodes at v = 0.2 V s^{-1}.

The irreversible character of peak *C* is indicative of instability of electrogenerated **21ē** complex $\mathbf{1}^-$, which, as is typical of nickelocene,[7] apparently decomposes with the destruction of the sandwich structure to form the (Ph)IndNi cryptoradical species, which are reduced more readily than the initial complex (the (the *ECE* scheme, where *E* and *C* are electrochemical and chemical stages, respectively). This is in agreement with the observed two-electron character of peak *C*. Although the nature of the products of the two-electron reduction of complex **1** was not studied in detail, metallic nickel and the $(Ph)Ind^-$ anion are most likely to be formed, as usually occurs during the two-electron reduction of metallocenes.[2,3,8] In turn, **19ē** cation $\mathbf{1}^+$ and **18ē** dication $\mathbf{1}^{2+}$ are stable, at least within the cyclic voltammetry time scale, which is evidenced by the quasi-reversible character of peaks *A*/*A′* and *B*/*B′*. Note that the stability of dication $\mathbf{1}^{2+}$, which exhibits strong electrophilic properties in the CH_2Cl_2 medium, qualitatively agree with the stability of the nickelocene dication,[9] and this is uncommon.[2,3]

Table 1. Potentials of the peaks in the cyclic voltammograms of complex **1** (CH_2Cl_2/0.05 mol L^{-1} Bu_4NPF_6) at different temperatures

Complex	Electrode	Peak	$E^0(E_p)$/sce	
			15 °C	−25 °C
1	Pt, GC*	*A*/*A′*	0.03	0.03
	Pt, GC	*B*/*B′*	0.80	0.80
	GC	*C*		−1.70
			15 °C	−58 °C
2	Pt	*D*/*D′*	−1.64	−1.64
	Pt	*E*		(−2.34)**
	Pt	*F*/*F′*		−2.47

* Glassy-carbon electrode. ** Irreversible peak.

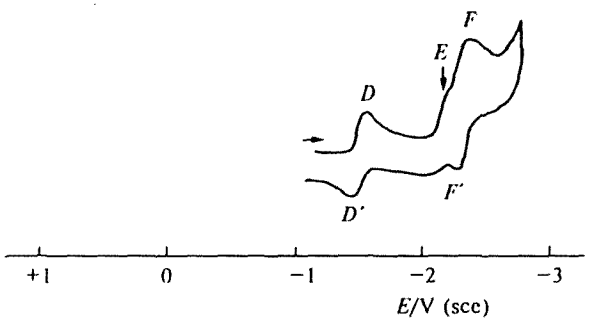

Fig. 5. Cyclic voltammogram of complex **2** ($1.2 \cdot 10^{-3}$ mol L^{-1}) in a THF solution/0.05 mol L^{-1} Bu_4NPF_6 on Pt-electrode (v = 0.2 V/s) at −58 °C.

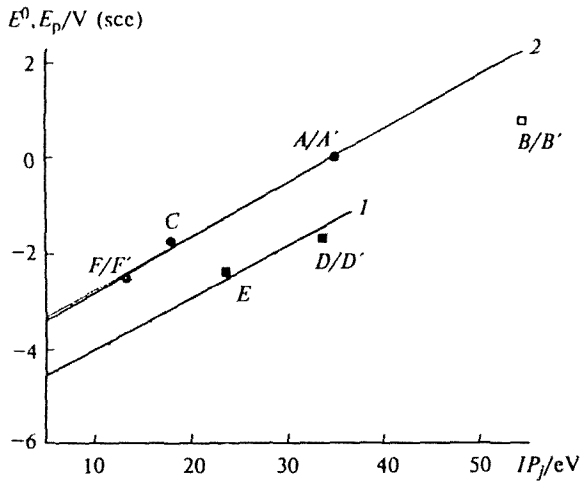

Fig. 6. Depenence between the values of E^0 and E_p for complexes **1**—**3** and the corresponding ionization potentials of metals (according to the data in Ref. 12): *1*, for bent-sandwich complex **2**; *2*, for sandwich complexes **1** and **3**.

The cyclic voltammograms of the $[\eta^5\text{-(Ph)Ind}]_2ZrCl_2$ complex (**2**) in the THF medium in the temperature range from −60 to +15 °C differ in some features, which are typical of biscyclopentadienyl dichloride complexes of Group IV metals.[4,5,7,8] The cyclic voltammogram of complex **2** at reduced temperatures (−45 °C) is the most informative, whereas at room temperature, the peak current of the complex is obscured by the discharge of the supporting electrolyte (Bu_4N^+). Figure 5 shows a typical cyclic voltammogram of complex **2** at −58 °C; all peaks are diffusion ($I_p \cdot v^{-1/2}$ = const) and one-electron, because they are comparable in height to the one-electron peak of reduction of the Cp^*ZrCl_2 complex (Cp^* is pentamethylcyclopentadienyl); these peaks were recorded under identical conditions. By analogy with the redox behavior of the substituted biscyclopentadienylzirconium dichlorides[10,11] studied previously, the quasi-reversible pair of peaks *D*/*D'* (ΔE_p = 90 and 60 mV at 15 and −38 °C, respectively) correspond to generation of radical anion $\mathbf{2}^{\cdot-}$, which is stable within the cyclic voltammetry time scale. Further reduction of $\mathbf{2}^{\cdot-}$ to dianion $\mathbf{2}^{2-}$ is chemically irreversible and is attended by the splitting out of two Cl^- ions to form 2-phenyl-substituted bisindenylzirconium $[\eta^5\text{-(Ph)Ind}]_2Zr$ (**3**). Compound **3** undergoes quasi-reversible (ΔE_p = 80 mV at −58 °C) one-electron reduction to the corresponding radical anion $\mathbf{3}^{\cdot-}$ at potentials of peak *F*; this radical anion is stable at −45 °C within the time scale of the method. Therefore, reduction of complex **2** proceeds according to the following scheme:

$$\mathbf{2} \underset{D/D'}{\overset{e}{\rightleftharpoons}} \mathbf{2}^{\cdot-} \underset{-E}{\overset{e,\,-2Cl^-}{\rightleftharpoons}} \mathbf{3} \underset{F/F'}{\overset{e}{\rightleftharpoons}} \mathbf{3}^{\cdot-}$$

Although isolation of intermediates $\mathbf{2}^{\cdot-}$, **3**, and $\mathbf{3}^{\cdot-}$ is impossible because of their instability, the suggested scheme of reduction of complex **2** is indirectly supported by the data presented in Fig. 6, which shows the relationship between the redox potentials $\Delta E^0 = (E^c_p + E^a_p)/2$ observed in the voltammograms of the peaks of complexes **1**—**3** and the corresponding gas-phase ionization potentials of the metals (IP_j). It is known[4,5,9—11] that for sandwich and bent-sandwich complexes of transition metals with the same ligands, unified linear relationships between the values of E^0 of all possible redox transformations of complexes and the values of IP_j of metals occur:

The slope of these dependences is close to 0.1 V eV^{-1}, regardless of the nature of the ligand, whereas the segment on the redox potential axis (Σa_i) intercepted by straight lines is determined by the nature of the π and s ligands. Then, taking the slope to be 0.1 V eV^-, two different linear $E^0(E_p)$—IP_j dependences should occur for the complexes studied in this work: one of these dependences (*1*) for bent-sandwich complex **2** (points *E* and *D*/*D'*; the notations of the points in Fig. 6 and the peaks in the voltammograms are the same) and the second dependence (*2*) for sandwich complexes **1** and **3** (points *A*/*A'*, *B*/*B'*, *C*, and *F*/*F'* in Fig. 4). Note that the deviation of point *B*/*B'* from linear dependence *2* toward more negative potentials should be observed because the electron is transferred to the antibonding orbital during reduction of complex $\mathbf{1}^{2+}$;[2,3,12—14] therefore, this point was ignored when curve *2* was constructed. Despite the small number of points, the fact that straight lines *1* and *2* in Fig. 6 are parallel to each other supports, in our opinion, the schemes of redox transformations of complexes **1** and **2** suggested above. The so-called constant of the ligand (a_i)[2,3,12—14] can be estimated from the length of the segment on the redox potential axis intercepted by straight line *2*; for $[\eta^5\text{-(Ph)Ind}]^-$, this constant is −1.93 V.

One more problem associated with the possible difference in redox properties of the *syn* and *anti* isomers of complexes **1** and **2** should be discussed. No difference in the redox behavior of these two isomers is observed within the accuracy of measurements of potentials (±0.01 V). This is determined by the close values of the energies of the frontier orbitals (HOMO and LUMO) on which electronic changes are located in redox reactions

Table 2. Atomic coordinates of nonhydrogen atoms ($\times 10^4$) in the structure of **1** and their equivalent isotropic temperature factors ($\times 10^3$)

Atom	*x*	*y*	*z*	*U*/Å
Ni(1)	5000	5000	0	29(1)
C(1)	3742(6)	5227(7)	695(3)	28(2)
C(2)	4754(6)	6182(8)	917(3)	28(2)
C(3)	4927(6)	7100(8)	415(3)	29(2)
C(4)	3886(6)	6847(8)	−117(3)	29(2)
C(5)	3258(7)	5525(9)	37(3)	36(2)
C(6)	3429(7)	4081(8)	1077(3)	36(2)
C(7)	4113(7)	3982(10)	1683(3)	43(2)
C(8)	5102(7)	4962(10)	1909(3)	42(2)
C(9)	5461(7)	6037(8)	1533(3)	35(2)
C(10)	3593(7)	7665(8)	−721(3)	31(2)
C(11)	4386(7)	8771(8)	−853(3)	34(2)
C(12)	4093(7)	9491(8)	−1437(3)	37(2)
C(13)	3037(7)	9149(9)	−1872(3)	42(2)
C(14)	2245(8)	8081(11)	−1736(4)	52(2)
C(15)	2500(6)	7322(9)	−1161(3)	36(2)
Ni(2)	10000	10000	0	32(1)
C(1′)	8838(6)	8751(7)	−933(3)	30(2)
C(2′)	8026(6)	9766(8)	−739(3)	33(2)
C(3′)	8186(6)	9498(8)	−80(3)	30(2)
C(4′)	8975(6)	8171(8)	99(3)	31(2)
C(5′)	9522(7)	7865(7)	−395(3)	30(2)
C(6′)	8889(8)	8801(9)	−1553(3)	43(2)
C(7′)	8156(8)	9824(11)	−1955(3)	51(2)
C(8′)	7382(7)	10840(10)	−1754(4)	48(2)
C(9′)	7331(7)	10813(9)	−1147(3)	43(2)
C(10′)	9289(6)	7390(8)	722(3)	30(2)
C(11′)	8640(7)	7783(9)	1146(3)	44(2)
C(12′)	8968(8)	7069(10)	1726(4)	50(2)
C(13′)	9890(8)	6022(10)	1872(4)	47(2)
C(14′)	10539(8)	5647(9)	1461(3)	43(2)
C(15′)	10231(7)	6299(8)	876(3)	41(2)

for two isomers. According to Hoffmann,[15] the energies of the frontiers orbitals for bent-sandwich complexes depend on the angle between aromatic π ligands (Ind—Zr—Ind). The values of these angles are very close for both isomers (131.6° and 131.2° for the *anti* and *syn* conformers, respectively). It is unlikely that a substantial difference in the energies of the HOMO and LUMO of the *syn* and *anti* isomers would occur for sandwich complex **1**. Because of this, splitting of the peaks was not observed in the voltammograms for complexes **1** and **2** throughout the temperature range studied.

Experimental

Toluene and THF freshly distilled over $LiAlH_4$ were used for preparing complexes **1** and **2**. All procedures were carried out under a pure argon atmosphere using the Schlenk technique.

Synthesis of $[\eta^5$-(Ph)Ind$]_2ZrCl_2$ (2). One equivalent of Bu^nLi (3 mL, 2 *M* in hexane, 6 mmol) was added dropwise with continuos stirring at −50 °C to a suspension of 2-phenylindene (2-PhInd, 1.146 g, 6 mmol) in 10 mL of toluene with a small amount of THF. The yellow-orange solution of 2-PhIndLi was slowly heated and kept for 2 h at room temperature. Then the solution was added dropwise with

Table 3. Atomic coordinates of nonhydrogen atoms ($\times 10^4$) in the structure of **2** and their equivalent isotropic temperature factors ($\times 10^3$)

Atom	*x*	*y*	*z*	*U*/Å
Zr(1)	1830(1)	6071(1)	2402(1)	27(1)
Cl(1)	1301(2)	5634(2)	1334(2)	42(1)
Cl(2)	1923(2)	4366(2)	3671(2)	41(1)
C(1)	−13(8)	8550(8)	1317(6)	40(2)
C(2)	−799(8)	8481(8)	1032(7)	45(3)
C(3)	−1376(8)	7717(8)	1642(7)	44(3)
C(4)	−1201(8)	7069(8)	2537(7)	41(3)
C(5)	−413(7)	7151(7)	2849(6)	30(2)
C(6)	208(7)	7884(7)	2241(6)	29(2)
C(7)	892(7)	7825(6)	2764(6)	31(2)
C(8)	678(7)	7070(6)	3713(5)	31(2)
C(9)	−56(7)	6595(7)	3740(6	33(2)
C(10)	1135(7)	6838(6)	4533(6)	29(2)
C(11)	1783(8)	7400(8)	4440(7)	43(3)
C(12)	2180(9)	7210(9)	5221(7)	48(3)
C(13)	1916(8)	6486(7)	6107(7)	40(2)
C(14)	1285(8)	5911(8)	6215(6)	48(3)
C(15)	891(7)	6084(7)	5423(6)	33(2)
C(16)	2987(8)	8063(8)	673(7)	48(3)
C(17)	2898(8)	8310(10)	−237(8)	56(3)
C(18)	3109(8)	7541(10)	−664(7)	60(3)
C(19)	3435(7)	6465(9)	−154(7)	48(3)
C(20)	3570(7)	6162(7)	813(6)	38(2)
C(21)	3327(7)	7007(7)	1213(6)	37(2)
C(22)	3537(7)	6463(7)	2187(6)	32(2)
C(23)	3948(7)	5379(7)	2335(6)	33(2)
C(24)	3915(7)	5171(8)	1506(6)	42(3)
C(25)	4367(6)	4535(7)	3178(7)	35(2)
C(26)	4176(9)	4817(9)	4019(7)	54(3)
C(27)	4528(9)	4006(10)	4825(8)	63(3)
C(28)	5076(9)	2968(9)	4808(9)	58(3)
C(29)	5303(9)	2702(9)	3962(9)	59(3)
C(30)	4945(8)	3494(8)	3158(8)	49(3)
Zr(2)	7277(1)	−1116(1)	8086(1)	23(1)
Cl(3)	6653(2)	760(2)	7200(2)	40(1)
Cl(4)	7457(2)	−836(2)	9458(1)	34(1)
C(31)	9389(7)	−3484(7)	8729(6)	34(2)
C(32)	9954(8)	−3464(8)	9280(6)	43(2)
C(33)	10325(8)	−2633(8)	9044(6)	39(2)
C(34)	10114(7)	−1731(7)	8261(6)	32(2)
C(35)	9533(6)	−1739(6)	7660(5)	27(2)
C(36)	9195(7)	−2634(7)	7892(6)	29(2)
C(37)	8724(6)	−2418(6)	7138(6)	28(2)
C(38)	8772(6)	−1427(7)	6432(5)	27(2)
C(39)	9220(6)	−972(6)	6803(5)	25(2)
C(40)	8462(7)	−932(7)	5495(5)	26(2)
C(41)	8247(7)	−1559(7)	5130(6)	30(2)
C(42)	7935(7)	−1091(8)	4247(6)	40(2)
C(43)	7856(7)	−69(8)	3728(6)	40(2)
C(44)	8085(7)	564(8)	4062(6)	38(2)
C(45)	8396(7)	91(7)	4950(6)	35(2)
C(46)	5871(8)	1537(8)	6934(6)	41(2)
C(47)	5187(9)	−599(10)	6442(7)	54(3)
C(48)	4456(9)	231(9)	6895(8)	53(3)
C(49)	4426(8)	169(8)	7822(6)	37(2)
C(50)	5113(7)	−745(7)	8326(6)	28(2)
C(51)	5836(7)	−1633(7)	7905(6)	31(2)
C(52)	6381(7)	−2492(6)	8613(5)	29(2)
C(53)	5959(7)	−2151(6)	9496(5)	25(2)
C(54)	5253(6)	−1055(7)	9279(6)	27(2)
C(55)	6215(7)	−2836(6)	10448(5)	29(2)
C(56)	5783(7)	−2382(7)	11238(6)	34(2)
C(57)	5965(8)	−3043(8)	12158(6)	41(2)
C(58)	6554(8)	−4089(9)	12291(7)	47(3)
C(59)	6990(8)	−4559(7)	11517(7)	50(3)
C(60)	6813(7)	−3910(7)	10601(6)	42(2)

Table 4. Bond lengths (Å) and the principal bond angles (ω) in the structure of **1**

Bond	d/Å	Bond	d/Å
Ni(1)—C(1)	2.397(7)	Ni(2)—C(1′)	2.418(7)
Ni(1)—C(2)	2.390(7)	Ni(2)—C(2′)	2.420(7)
Ni(1)—C(3)	2.048(7)	Ni(2)—C(3′)	2.068(8)
Ni(1)—C(4)	2.006(7)	Ni(2)—C(4′)	2.006(7)
Ni(1)—C(5)	2.056(8)	Ni(2)—C(5′)	2.052(6)
C(1)—C(2)	1.393(9)	C(1′)—C(6′)	1.416(9)
C(1)—C(6)	1.418(9)	C(1′)—C(2′)	1.423(9)
C(1)—C(5)	1.461(9)	C(1′)—C(5′)	1.468(9)
C(21—C(9)	1.413(9)	C(2′)—C(9′)	1.378(10)
C(2)—C(3)	1.437(9)	C(2′)—C(3′)	1.468(9)
C(3)—C(4)	1.460(9)	C(3′)—C(4′)	1.441(9)
C(4)—C(5)	1.435(9)	C(4′)—C(5′)	1.441(9)
C(4)—C(10)	1.491(9)	C(4′)—C(10′)	1.512(9)
C(6)—C(7)	1.383(10)	C(6′)—C(7′)	1.374(11)
C(7)—C(8)	1.388(11)	C(7′)—C(8′)	1.399(11)
C(8)—C(9)	1.389(10)	C(8′)—C(9′)	1.387(10)
C(10)—(11)	1.398(9)	C(10′)—C(15	1.396(10)
C(10)—C(15)	1.400(9)	C(10′)—C(11)	1.398(10)
C(11)—C(12)	1.413(9)	C(11′)—C(12)	1.404(11)
C(12)—C(13)	1.363(10)	C(12′)—C(13′)	1.355(11)
C(13)—C(14)	1.377(11)	C(13′)—C(14′)	1.371(10)
C(14)—C(15)	1.412(10)	C(14)—C(15)	1.390(10)

Angle	ω/deg	Angle	ω/deg
C(2)—C(1)—C(6)	120.6(6)	C(6′)—C(1′)—C(2′)*	119.2(7)
C(2)—C(1)—C(5)	108.2(6)	C(6′)—C(1′)—C(5′)	132.8(7)
C(6)—C(1)—C(5)	130.8(6)	C(2′)—C(1′)—C(5′)	107.9(6)
C(1)—C(2)—C(3)	108.4(6)	C(9′)—C(2′)—C(1′)	119.9(6)
C(9)—C(2)—C(3)	131.4(6)	C(9′)—C(2′)—C(3′)	132.4(7)
C(1)—C(2)—C(9)	120.0(6)	C(1′)—C(2′)—C(3′)	107.6(6)
C(2)—C(3)—C(4)	108.3(6)	C(4′)—C(3′)—C(2′)	107.9(6)
C(5)—C(4)—C(10)	126.4(6)	C(5′)—C(4′)—C(3′)	107.1(6)
C(3)—C(4)—C(10)	128.0(6)	C(5′)—C(4′)—C(10′)	126.5(7)
C(5)—C(4)—C(3)	105.4(6)	C(3′)—C(4′)—C(10′)	125.9(6)
C(4)—C(5)—C(1)	108.0(6)	C(4′)—C(5′)—C(1′)	107.6(6)
C(7)—C(6)—C(1)	118.6(7)	C(9′)—C(8′)—C(7′)	120.4(8)
C(6)—C(7)—C(8)	120.8(7)	C(2′)—C(9′)—C(8′)	120.3(8)
C(7)—C(8)—C(9)	121.5(7)	C(15′)—C(10′)—C(11′)	120.2(7)
C(8)—C(9)—C(2)	118.4(7)	C(15′)—C(10′)—C(4′)	120.3(6)
C(11)—C(10)—C(15)	119.5(6)	C(11′)—C(10′)—C(4′)	119.5(7)
C(11)—C(10)—C(4)	121.2(6)	C(10′)—C(11′)—C(12′)	118.5(8)
C(15)—C(10)—C(4)	119.2(6)	C(13′)—C(12′)—C(11′)	120.8(8)
C(10)—C(11)—C(12)	119.6(7)	C(12′)—C(13′)—C(14′)	121.0(8)
C(13)—C(12)—C(11)	121.2(7)	C(13′)—C(14′)—C(15′)	120.3(8)
C(12)—C(13)—C(14)	119.1(7)	C(14′)—C(15′)—C(10′)	119.3(7)

* The second independent molecule.

continuos stirring to a suspension of $ZrCl_4$ (Aldrich, 0.67 g, 3 mmol) in toluene at −15 °C. The temperature of the reaction mixture was raised to room temperature, and the lemon-yellow solution with a yellow precipitate was stirred for 8 h. Then the solvent was removed by distillation *in vacuo*, $[\eta^5\text{-(Ph)Ind}]_2ZrCl_2$ was extracted repeatedly with toluene, and the extracts were combined, concentrated by removing a portion of the solvent *in vacuo*, and cooled to −30 °C. The crystals that formed were washed with cold pentane and dried *in vacuo*. The yield of compound **2** was 1.4 g (86 %). Found (%): C, 50.92; H, 3.08; Cl, 20.12; Zr 25.78. Calculated (%): C, 50.98; H, 3.14; Cl, 20.07; Zr, 25.81. Single crystals suitable for X-ray structural study were obtained by recrystallization of **2** from a 1 : 1 (volume) toluene : THF mixture. To perform X-ray structural analysis, a crystal of **2** of dimensions about 0.4 mm was placed in a 0.7 mm-diameter capillary and sealed with picein.

Synthesis of $[\eta^5\text{-(Ph)Ind}]_2Ni$ (1) was performed starting from $NiBr_2$ (Aldrich) and 2-phenylindenyllithium under conditions analogous to those used in the synthesis of **2**. The yield of **1** was 75 %. Bright-red crystals of $[\eta^5\text{-(Ph)Ind}]_2Ni$ readily soluble in THF, CH_2Cl_2, and toluene were obtained. Found (%): C, 72.12; H, 4.48; Ni, 23.42. Calculated: C, 72.08; H, 4.44; Ni, 23.48.

X-Ray diffraction analysis of compounds **1** and **2** was carried out at −81 °C on an automated four-circle Syntex $P2_1$

Table 5. Bond lengths (Å) in the structure of **2**

Bond	*d*/Å	Bond	*d*/Å	Bond	*d*/Å	Bond	*d*/Å
Zr(1)—Cl(1)	2.422(2)	Zr(2)—Cl(4)	2.427(2)	C(10)—C(15)	1.379(11)	C(40)—C(45)	1.363(11)
Zr(1)1—Cl(2)	2.442(2)	Zr(2)—Cl(3)	2.430(2)	C(10)—C(11)	1.380(11)	C(40)—C(41)	1.424(11)
Zr(1)—C(7)	2.467(8)	Zr(2)—C(37)	2.459(7)	C(11)—C(12)	1.396(12)	C(41)—C(42)	1.399(12)
Zr(1)—C(22)	2.479(8)	Zr(2)—C(52)	2.482(8)	C(12)—C(13)	1.359(13)	C(42)—C(43)	1.351(12)
Zr(1)—C(8)	2.507(7)	Zr(2)—C(51)	2.529(8)	C(13)—C(14)	1.366(13)	C(43)—C(44)	1.410(12)
Zr(1)—C(9)	2.530(7)	Zr(2)—C(36)	2.538(8)	C(14)—C(15)	1.417(12)	C(44)—C(45)	1.404(11)
Zr(1)—C(24)	2.536(8)	Zr(2)—C(38)	2.552(7)	C(16)—C(17)	1.338(14)	C(46)—C(47)	1.381(14)
Zr(1)—C(23)	2.545(8)	Zr(2)—C(54)	2.554(7)	C(16)—C(21)	1.383(13)	C(46)—C(51)	1.423(11)
Zr(1)—C(6)	2.564(8)	Zr(2)—C(39)	2.571(7)	C(17)—C(18)	1.38(2)	C(47)—C(48)	1.397(14)
Zr(1)—C(21)	2.571(8)	Zr(2)—C(53)	2.573(7)	C(18)—C(19)	1.391(14)	C(48)—C(49)	1.373(13)
Zr(1)—C(20)	2.581(7)	Zr(2)—C(50)	2.614(8)	C(19)—C(20)	1.436(13)	C(49)—C(50)	1.377(12)
Zr(1)—C(5)	2.644(8)	Zr(2)—C(35)	2.622(8)	C(20)—C(24)	1.413(12)	C(50)—C(54)	1.415(11)
C(1)—C(2)	1.364(12)	C(31)—C(32)	1.374(12)	C(20)—C(21)	1.443(12)	C(50)—C(51)	1.434(11)
C(1)—C(6)	1.423(12)	C(31)—C(36)	1.398(12)	C(21)—C(22)	1.463(12)	C(51)—C(52)	1.427(11)
C(2)—C(3)	1.428(14)	C(32)—C(33)	1.371(12)	C(22)—C(23)	1.369(11)	C(52)—C(53)	1.431(10)
C(3)—C(4)	1.363(13)	C(33)—C(34)	1.386(12)	C(23)—C(24)	1.446(11)	C(53)—C(54)	1.427(11)
C(4)—C(5)	1.403(12)	C(34)—C(35)	1.450(11)	C(23)—C(25)	1.487(12)	C(53)—C(55)	1.478(11)
C(5)—C(6)	1.430(12)	C(35)—C(39)	1.417(11)	C(25)—C(30)	1.366(12)	C(55)—C(60)	1.372(11)
C(5)—C(9)	1.439(12)	C(35)—C(36)	1.432(11)	C(25)—C(26)	1.399(12)	C(55)—C(56)	1.398(10)
C(6)—C(7)	1.419(11)	C(36)—C(37)	1.412(11)	C(26)—C(27)	1.399(14)	C(56)—C(57)	1.400(11)
C(7)—C(8)	1.428(11)	C(37)—C(38)	1.418(11)	C(27)—C(28)	1.36(2)	C(57)—C(58)	1.339(13)
C(8)—C(9)	1.423(11)	C(38)—C(39)	1.446(10)	C(28)—C(29)	1.378(14)	C(58)—C(59)	1.391(13)
C(8)—C(10)	1.487(11)	C(38)—C(40)	1.471(11)	C(29)—C(30)	1.392(14)	C(59)—C(60)	1.389(12)

Table 6. Principal bond angles (ω) in the structure of **2**

Angle	ω/deg	Angle	ω/deg	Angle	ω/deg
Cl(1)—Zr(1)—Cl(2)	94.54(9)	C(16)—C(21)—C(20)	120.6(9)	C(35)—C(39)—C(38)	107.8(7)
C(2)—C(1)—C(6)	120.1(9)	C(16)—C(21)—C(22)	134.5(9)	C(45)—C(40)—C(41)	118.5(8)
C(1)—C(2)—C(3)	120.3(9)	C(20)—C(21)—C(22)	104.8(8)	C(45)—C(40)—C(38)	123.0(7)
C(4)—C(3)—C(2)	121.6(10)	C(23)—C(22)—C(21)	110.3(8)	C(41)—C(40)—C(38)	118.5(7)
C(3)—C(4)—C(5)	118.6(9)	C(22)—C(23)—C(24)	107.8(8)	C(42)—C(41)—C(40)	118.9(8)
C(4)—C(5)—C(6)	121.3(8)	C(22)—C(23)—C(25)	128.0(8)	C(42)—C(43)—C(44)	120.7(9)
C(4)—C(5)—C(9)	131.5(8)	C(20)—C(24)—C(23)	107.9(8)	C(43)—C(44)—C(45)	117.5(9)
C(6)—C(5)—C(9)	107.2(8)	C(25)—C(30)—C(29)	122.0(10)	C(40)—C(45)—C(44)	122.8(9)
C(7)—C(6)—C(5)	108.7(8)	C(30)—C(25)—C(26)	118.7(9)	C(47)—C(46)—C(51)	118.7(9)
C(7)—C(6)—C(1)	133.1(8)	C(30)—C(25)—C(23)	122.3(9)	C(46)—C(47)—C(48)	120.9(9)
C(5)—C(6)—C(1)	118.1(8)	C(26)—C(25)—C(23)	119.0(8)	C(49)—C(48)—C(47)	121.6(10)
C(6)—C(7)—C(8)	107.6(7)	C(27)—C(26)—C(25)	118.3(10)	C(48)—C(49)—C(50)	119.1(9)
C(9)—C(8)—C(7)	108.4(7)	C(28)—C(27)—C(26)	122.6(11)	C(49)—C(50)—C(54)	132.4(8)
C(9)—C(8)—C(10)	126.2(7)	C(27)—C(28)—C(29)	118.8(11)	C(49)—C(50)—C(51)	120.9(8)
C(7)—C(8)—C(10)	125.4(8)	C(28)—C(29)—C(30)	119.5(10)	C(54)—C(50)—C(51)	106.7(7)
C(8)—C(9)—C(5)	107.6(8)	Cl(4)—Zr(2)—Cl(3)	95.75(8)	C(46)—C(51)—C(50)	118.7(8)
C(15)—C(10)—C(11)	117.9(8)	C(32)—C(31)—C(36)	119.0(9)	C(52)—C(51)—C(50)	108.9(7)
C(15)—C(10)—C(8)	121.3(8)	C(31)—C(32)—C(33)	122.3(9)	C(53)—C(52)—C(51)	107.4(7)
C(11)—C(10)—C(8)	120.8(8)	C(32)—C(33)—C(34)	122.5(9)	C(52)—C(53)—C(54)	107.3(7)
C(10)—C(11)—C(12)	121.0(9)	C(33)—C(34)—C(35)	116.1(8)	C(52)—C(53)—C(55)	125.0(7)
C(13)—C(12)—C(11)	121.1(10)	C(39)—C(35)—C(36)	109.0(7)	C(54)—C(53)—C(55)	127.7(7)
C(14)—C(13)—C(12)	119.0(9)	C(39)—C(35)—C(34)	130.5(8)	C(50)—C(54)—C(53)	109.3(7)
C(13)—C(14)—C(15)	120.5(9)	C(36)—C(35)—C(34)	120.5(8)	C(60)—C(55)—C(56)	118.7(8)
C(10)—C(15)—C(14)	120.5(9)	C(31)—C(36)—C(37)	134.5(8)	C(60)—C(55)—C(53)	122.4(7)
C(17)—C(16)—C(21)	120.1(10)	C(31)—C(36)—C(35)	119.3(8)	C(56)—C(55)—C(53)	118.8(7)
C(16)—C(17)—C(18)	122.4(11)	C(37)—C(36)—C(35)	106.2(7)	C(57)—C(56)—C(55)	118.8(8)
C(17)—C(18)—C(19)	120.4(10)	C(38)—C(37)—C(36)	110.7(7)	C(58)—C(57)—C(56)	121.5(8)
C(18)—C(19)—C(20)	119.0(9)	C(37)—C(38)—C(39)	106.0(7)	C(57)—C(58)—C(59)	120.7(9)
C(24)—C(20)—C(19)	133.8(9)	C(37)—C(38)—C(40)	129.0(7)	C(60)—C(59)—C(58)	118.2(9)
C(24)—C(20)—C(21)	108.9(8)	C(39)—C(38)—C(40)	125.0(7)	C(55)—C(60)—C(59)	122.0(8)

diffractometer (Mo-Kα radiation, Nb filter, θ/2θ scanning technique, $2\theta < 54°$). The crystals of **1** are monoclinic, at −81 °C: a = 11.37(2) Å, b = 8.606(9) Å, c = 22.58(3) Å, β = 105.55(5)°, V = 2129(5) Å^3, space group $P2_1/n$, Z = 2, d_{calc} = 1.376 g cm^{-3}, μ = 0.926 cm^{-1}. The crystals of **2** are triclinic, at −81 °C: a = 13.533(5) Å, b = 14.557(6) Å, c = 15.363(5) Å, α = 65.97(2)°, β = 64.92(2)°, γ = 63.33(1)°, V = 2360(2) Å^3, M = 544.59, $C_{60}H_{44}Cl_4Zr_2$, space group

$P\bar{1}$, $Z = 2$, $d_{calc} = 1.533$ g cm^{-3}, $\mu = 7.09$ cm^{-1}. Of a total of 5020 and 7040 measured reflections in the structures of **1** and **2**, respectively, 4010 and 6804 independent reflections were used in calculations. The structures were solved by the direct method and refined anisotropically by the full-matrix least-squares method. The positions of hydrogen atoms were determined from geometric considerations and refined using the riding model with fixed thermal parameters. Absorption corrections were applied using the DIFABS program. All calculations were performed on an IBM-PC/AT computer using the SHLXTL program (Version 5). The final values of R factors are as follows: $R = 0.0816$ based on 1672 reflections with $I > 2\sigma(I)$, $wR1 = 0.1544$, GOF = 0.975 based on all reflections, and R = 0.070 based on 4077 reflections with $I > 2\sigma(I)$, $wR1 = 0.1436$ based on all reflections in the structures of **1** and **2**, respectively. Atomic coordinates of nonhydrogen atoms in the structures of **1** and **2** and their isotropic temperature factors are given in Tables 2 and 3, respectively; bond lengths and bond angles are listed in Tables 4 and 6.

Voltammetric measurements were carried out under a dry argon atmosphere in solvents that had been prepurified and distilled directly into an electrochemical cell (evacuated and filled with argon), according to the procedure described previously.[16] THF (Aldrich) was purified by the ketyl method; CH_2Cl_2 (Aldrich) was purified by boiling over P_2O_5. A Bu_4NPF_6 (0.05 *M*) solution was used as the supporting electrolyte. Tetrabutylammonium hexafluorophosphate (Aldrich) was preliminarily dehydrated by melting *in vacuo*. Low-temperature electrochemical measurements were performed using a cell thermostatically controlled with ethanol, which was cooled with liquid nitrogen in a Dewar vessel.

All measured potentials are given relative to an aqueous saturated calomel electrode by comparing the potential of the reference electrode (an Ag/AgCl/4 *M* aqueous solution of LiCl), which was separated from the solution studied by a bridge filled with a solution of the supporting electrolyte, with the potential of the redox transformation of decamethylferrocene$^{0/+}$ ($E^0 = 0/00$ V, saturated calomel electrode in THF and -0.10 V in CH_2Cl_2).

A 1-mm disk platinum electrode or a glassy-carbon electrode (3 mm; Tokai, Japan) sealed into glass and polished off with diamond paste (the grain size was ≤ 1 μm) were used as working electrodes. Voltammeric measurements were carried out using a PAR 175 generator of signals and a PAR 173 potentiostat with compensation of ohmic losses. Voltammograms were recorded on a two-coordinate RE0074 recorder.

This work was financially supported by the Russian Foundation for Basic Research (Project Nos. 95-03-09836a and 93-04-07252) and the International Science Foundation (Grant REV 300).

References

1. G. W. Coates and R. M. Waymouth, *Science*, 1995, **267**, 217.
2. V.V. Strelets, *Usp. Khim.*, 1989, **58**, 496 [*Russ. Chem. Rev.*, 1989, **58** (Engl. Transl.)].
3. V. V. Strelets, *Coord. Chem. Rev.*, 1992, **114**, 1.
4. S. V. Kukharenko, V. V. Strelets, M. G. Peterleiter, L. I. Denisovich, A. R. Kudinov, A. Z. Kreidlin, and M. I. Rybinskaya, *Izv. Akad. Nauk, Ser. Khim.*, 1995, 2394 [*Russ. Chem. Bull.*, 1995, **44**, 2289 (Engl. Transl.)].
5. P. M. Treichel, and J. M. Jonson, *J. Organomet. Chem.*, 1975, **88**, 207.
6. S. V. Kukharenko, V. V. Strelets, N. A. Ustynyuk, L. N. Novikova, L. I. Denisovich, and M. G. Peterleitner, *Metalloorg. Khim.*, 1991, **4**, 299 [*Organomet. Chem. USSR*, 1991, **4** (Engl. Transl.)].
7. J. D. Payne and N. El Murr, *J. Am. Chem. Soc. Chem. Commun.*, 1984, 1137.
8. S. V. Kukharenko, E. M. Koldasheva, and V. V. Strelets, *Dokl. Akad. Nauk SSSR*, 1988, **303**, 112 [*Dokl. Chem.*, 1988, **303** (Engl. Transl.)].
9. R. J. Wilson, L. F. Warren, and M. F. Hawthorne, *J. Am. Chem. Soc.*, 1969, **91**, 758.
10. S. V. Kukharenko, G. L. Soloveichik, and V. V. Strelets, *Metalloorg. Khim.*, 1989, **2**, 395 [*Organomet. Chem. USSR*, 1989, **2** (Engl. Transl.)].
11. G. L. Soloveichik, A. B. Gavrilov, and V. V. Strelets, *Metalloorg. Khim.*, 1989, **2**, 431 [*Organomet. Chem. USSR*, 1989, **2** (Engl. Transl.)].
12. V. V. Strelets and S. V. Kukharenko, *Dokl. Akad. Nauk SSSR*, 1984, **275**, 894 [*Dokl. Chem.*, 1984, **275** (Engl. Transl.)].
13. V. V. Strelets and S. V. Kukharenko, *Nouv. J. Chim.*, 1984, **8**, 785.
14. V. V. Strelets and S. V. Kukharenko, *Metalloorg. Khim.*, 1988, **1**, 692 [*Organomet. Chem. USSR*, 1988, **1** (Engl. Transl.)].
15. J. W. Lauher and R. Hoffman, *J. Am. Chem. Soc.*, 1978, **98**, 1729.
16. V. V. Strelets and K. Dzh. Pikket, *Elektrokhimiya*, 1994, **30**, 1023 [*Russ. J. Electrochem.*, 1994, **30** (Engl. Transl.)].

Received December 25, 1995;
in revised form April 5, 1996